Since January 2020 Elsevier has created a COVID-19 resource centre with free information in English and Mandarin on the novel coronavirus COVID-19. The COVID-19 resource centre is hosted on Elsevier Connect, the company's public news and information website.

VIROLOGY 214, 128–138 (1995)

A Conserved Motif at the 3′ End of Mouse Hepatitis Virus Genomic RNA Required for Host Protein Binding and Viral RNA Replication

WEI YU*,[1] and JULIAN L. LEIBOWITZ†,[2]

*Department of Pathology and Laboratory Medicine, The University of Texas Medical School at Houston, Houston, Texas 77030; and †Department of Pathology and Laboratory Medicine, 208 Reynolds Building, Texas A&M University College of Medicine, College Station, Texas 77843-1114

Received August 2, 1995; accepted September 18, 1995

A conserved 11-nucleotide sequence, UGAAUGAAGUU, at the 3′ end of the genomic RNA of coronavirus mouse hepatitis virus was required for host protein binding and viral RNA synthesis. An RNA probe containing this 11-nucleotide sequence bound four cellular proteins with a highly labeled protein of 120 kDa and three minor species with sizes of 103, 81, and 55 kDa. Mutation of the 11-nucleotide motif abolished cellular protein binding. The RNA–protein complexes observed with cytoplasmic extracts from MHV-JHM-infected cells in both RNase protection/gel mobility shift and UV cross-linking assays were indistinguishable from those observed with extracts from uninfected cells. Both negative-strand synthesis and positive-strand replication of viral defective interfering RNAs in the presence of helper virus were affected by mutations that disrupt RNA–protein complex formation, even though the 11 mutated nucleotides were converted to the wild-type sequence, presumably by recombination with helper virus. Kinetic analysis indicated that recombination between DI RNA and helper virus occurred relatively early in the MHV replicative cycle at 5.5 to 7.5 hr postinfection, a time when viral RNA synthesis and replication of positive-strand DI RNA were at barely detectable levels. A DI RNA with a mutation upstream of the protein binding element replicated as efficiently as wild type without undergoing recombination. Thus, the 11-nucleotide conserved host protein binding motif appears to play an important role in viral RNA replication.

INTRODUCTION

Mouse hepatitis virus (MHV), a coronavirus, contains a large, single-stranded, and polyadenylated genomic RNA of positive sense which is approximately 31 kb in length. Coronaviruses utilize a complex transcriptional strategy which is not completely understood. During the MHV replicative cycle, seven or eight species of virus-specific RNAs of positive polarity are synthesized, the largest of which corresponds to the genomic RNA, while the smaller subgenomic RNAs comprise a 3′-coterminal nested-set (Lai, 1990; Lai *et al.,* 1981; Leibowitz *et al.,* 1981, 1990; Spaan *et al.,* 1982). All of these positive-sense RNAs also contain a 70- to 75-nucleotide leader sequence at their 5′ termini which is identical to the sequence of genomic RNA at the 5′ end. Several models of discontinuous transcription have been described to explain the mechanism of MHV RNA synthesis (Brian *et al.,* 1994; Lai, 1990; Leibowitz *et al.,* 1990; Sawicki and Sawicki, 1990; Schaad and Baric, 1994; Spaan *et al.,* 1988). In all of these models, the initial step in MHV RNA replication is the synthesis of negative-strand RNA from a positive-strand genomic template. Thus, transcription of negative-strand RNA is a crucial event in viral replication. If this event is blocked, virus replication will not proceed past the translation of input viral genomic RNA.

Analysis of the structure of coronavirus defective interfering (DI) RNAs (naturally occurring or constructed *in vitro*) indicated that at least 436 nucleotides (nt) at the 3′ terminus are required for DI RNA replication (Kim *et al.,* 1993; Lin and Lai, 1993). Moderate deletions within the 436 nt at the 3′ end of the genome were lethal to DI RNA replication, suggesting that these sequences contain signals essential for RNA replication (Kim *et al.,* 1993). Further studies have demonstrated that only 55 nt at the 3′ terminus are required for negative-strand RNA synthesis in MHV-infected cells (Lin *et al.,* 1994). The sequences from 56 to 436 upstream of the 3′ terminus of the genome [excluding the poly(A) tail] are thought to play a role in the synthesis of plus-stranded RNA, although the mechanism by which this occurs is not clear.

Our approach to studying MHV RNA replication is to identify the *cis*-acting signals for RNA replication and the proteins which recognize these signals at the 3′ end of genomic RNA of MHV. We have focused our attention on the 3′ end of MHV genome as it is likely that the 3′ region contains sequences necessary for viral RNA polymerase binding, either alone or in combination with host proteins. We have recently reported the specific binding of multiple host cell proteins to two distinct sites within 487 nt at the 3′ end of genomic RNA of MHV. The first binding element was mapped within the 3′ most 42

[1] Current address: Department of Pathology and Laboratory Medicine, 208 Reynolds Building, Texas A&M University College of Medicine, College Station, TX 77843-1114.

[2] To whom correspondence and reprint requests should be addressed. Fax: (409) 862-1299. E-mail: jleibow@tam2000.tamu.edu.

0042-6822/95 $12.00

nt of the genomic RNA, while the second element was located within an 86-nt sequence encompassing nt 171 to 85 from the 3′ end of the genome (Yu and Leibowitz, 1995). Comparison of the sequences of two protein-binding elements revealed about 42% sequence identity with the sequence UGARNGAAGUU being present in both elements.

In this work we more precisely localize the sequence contributing to host protein binding to the last 42 nt at the 3′ end of the genome, again using RNase T_1 protection/gel mobility shift electrophoresis and UV-induced cross-linking assays. RNAs containing deletions or clustered-point mutations within the conserved 11-nt sequence (UGAAUGAAGUU) were tested for the ability to form complexes with uninfected and MHV, strain JHM (MHV-JHM)-infected cytoplasmic extracts. To investigate a possible role of this 3′ protein-binding element in viral RNA replication, DI RNAs containing mutations within the 11-nt motif were transcribed *in vitro* and transfected into permissive 17Cl-1 cells in the presence of MHV-JHM helper virus. The replication of positive-strand DI RNA as well as the transcription of negative-strand DI RNA were assayed to determine if such mutations affected either one or both of these steps in RNA synthesis. Here we report the identification of an 11-nt conserved motif (UGAAUGAAGUU) spanning nt 36 to 26 from the 3′ end of genomic RNA of MHV required for the specific binding of host cellular proteins and for the synthesis of both positive and negative DI RNAs.

MATERIALS AND METHODS

Virus and cells

Murine 17Cl-1 cells (a spontaneously transformed 3T3 Balb/c mouse fibroblast cell line) and MHV-JHM were used throughout this study as previously described (Yu and Leibowitz, 1995). DME was buffered to pH 7.3–7.4 with 15 m*M* each HEPES, MOPS, and TES.

Preparation of mock- and MHV-JHM-infected cytoplasmic extracts

Cytoplasmic extracts from both uninfected- and virus-infected cells were prepared as previously described (Yu and Leibowitz, 1995).

Design of primers and *in vitro* synthesis of RNA transcripts

PCR was utilized to synthesize cDNA fragments representing the 3′ end of the JHM genome under the control of the T7 RNA polymerase promoter. The 5′ primer containing the T7 RNA polymerase promoter (PT7-CCT GGG AAG AGC TCA CAT), fused to 18 nt starting at nt 84 from the 3′ end of genomic RNA (positive sense) was synthesized. The sequence of the 5′ primer for probe 3′ (+) 42, which also contains the T7 promoter fused to 18 nt starting at nt 42 from the 3′ end of genomic RNA, is PT7-TAG TAA ATG AAT GAA GTT. A series of 3′ end negative-sense primers with deletions or clustered-point mutations (underlined) were also synthesized as listed in Table 1.

TABLE 1

Probes and Primers Synthesized

Probes	Negative-sense 3′ primer
3′(+)42	GTG ATT CTT CCA ATT GGC
84-43	GGG CAT TGC AGG AAT AGT A
84-34	TCA TTT ACT AGG GCA TTG
84-24	TCA ACT TCA TTC ATT TAC
84-14	TTG GCC ATG ATC AAC TTC
84-16	GGC CAT GAT CAA CTT CAT TCA TTT
mB4	GGC CAT GAT CAA CTT CAT AGT TTT
mC5	GGC CAT GAT CTT GAA GAT TCA TTT
mF0	GGC CAT GAT CTT GAA GAT AGT TTT
mI	GGC CAT GAT CAA CTT CTA AGT TTT
mG1	GGC CAT GAT CTT GAA GTA AGT TTT

A double-stranded cDNA representing 487 nt from the 3′ end of JHM genomic RNA was used as a DNA template for PCR (Yu and Leibowitz, 1995). PCR products with defined sizes and mutations were synthesized by *Taq* DNA polymerase (Perkin–Elmer Cetus), purified by gel electrophoresis, and recovered from the gel using glass powder (Mermaid kit, Bio 101). Direct sequencing of PCR fragments was performed to confirm the identity of certain mutations. *In vitro* transcription reactions of PCR product templates by T7 polymerase were carried out as previously described (Yu and Leibowitz, 1995).

RNase T_1 protection/gel mobility shift electrophoresis assays and UV-induced cross-linking of RNA–protein complexes

The RNA–protein binding reaction and UV cross-linking of labeled RNA to protein were performed as previously described (Yu and Leibowitz, 1995). RNA–protein complex formation was quantitated by scanning the ^{32}P-labeled gels with a Betascope 603 blot analyzer (Betagen, Intelligenetics, Inc).

Construction of mutant DI cDNAs

cDNA mutants were constructed as described by the manufacturer using the Chameleon double-stranded, site-directed mutagenesis kit (Stratagene) according to the manufacturer's instructions. DE25, a 2.2-kb DIssE cDNA clone of the MHV-JHM DI RNA (Makino and Lai, 1989), was used as the target for site-directed mutagenesis. The synthetic selection and mutagenic primers designed to introduce clustered-point transversion mutations into the 11-nt protein-binding element or at selected sites within this element are listed below. The selection primer (5′-GCG CGA GGC CCA GAA CGT TAA TAC GAC

TCA CTA TAG-3′) was positive sense and destroys the unique *Hin*dIII restriction site upstream of the 5′ end of DE25 (Makino and Lai, 1989). The mutagenic primers were also positive sense and encoded the various mutations we desired to introduce into DE25 in the region responsible for host cellular protein binding. The sequence of mutagenic primer of mG1 DI RNA was 5′-CTG CAA TGC CCT AGT AAA ACT TAC TTC AAG ATC ATG GCC-3′, of mB4 DI RNA 5′-CTG CAA TGC CCT AGT AAA ACT ATG AAG TTG ATC ATG GCC-3′, of mC5 DI RNA 5′-GCC CTA GTA AAT GAA TCT TCA AGA TCA TGG CCA ATT GG-3′, and of mD6 DI RNA 5′-GTT GTG GCA GAC CCT GAT ACA ATT AGT TGA AAG AG-3′. The alterations from the wild-type MHV sequence are underlined. Each clone was sequenced to confirm the presence of the introduced mutation.

DI RNA transcription, transfection, and radiolabeling

Plasmid DNAs were linearized by *Xba*I digestion and transcribed with T7 RNA polymerase following a previously described procedure with some minor modifications (Soe *et al.,* 1987). After incubation for 90 to 120 min, the transcription reaction mixtures were treated with 3 units of RNase-free DNase (Ambion) and extracted twice with phenol/chloroform. Unincorporated nucleotides were removed by gel filtration through a Sephadex G-50 column (Sigma). DI RNAs were introduced into cells by liposome-mediated transfection following a previously described procedure except that cellFECTIN (Life Technologies) was used rather than lipofectin (Makino *et al.,* 1991). Monolayer cultures of murine 17Cl-1 cells in 35-mm six-well plates ($\sim 2.5 \times 10^6$ cells/well) were first infected with MHV-JHM at a multiplicity of infection of 5. After 1 hr of virus adsorption, the inoculum was removed and cells were washed twice with prewarmed serum-free DME medium. For each well, 1.5 μg of *in vitro* synthesized DI RNA was incubated with 15 μg of cellFECTIN in 0.4 ml serum-free DME for 15 min at room temperature and then added to the virus-infected cells. After incubation at 37° for 1 hr, 1.5 ml of prewarmed DME was added and the cultures incubated for another hour. The cellFECTIN-containing media were replaced with 3 ml of DME containing 2% FBS and incubated for an additional 3.5 to 4 hr. Cells were washed once with prewarmed phosphate-free DME, incubated for 20 min in 1 ml phosphate-free DME containing 10 μg/ml actinomycin D (Calbiochem), and then labeled with 200 μCi/ml ^{32}Pi (ICN) at 37° for 2 hr (7.5 to 9.5 hr postinfection) in the presence of actinomycin D until MHV-induced cytopathic effect (cell fusion) involved over 90% of the cells.

Detection of positive-strand DI RNA replication by agarose gel electrophoresis

^{32}P-labeled MHV-specific intracellular RNAs were extracted as previously described with some minor modifications (Leibowitz and DeVries, 1988). Briefly, the cells were washed twice with cold PBS, dissolved in 700 μl of cell lysis buffer containing 8 *M* guanidium hydrochloride, 0.1 *M* 2-mercaptoethanol, and 0.2 *M* sodium acetate, pH 5.0, and then the DNA was sheared by passage through a hypodermic needle. One-half volume of ethanol was added to the extract, the mixture was split into two aliquots containing one-third and two-thirds of the sample, and the RNA was allowed to precipitate at −20° over 2 hr. The aliquot containing one-third of the original sample was analyzed directly by agarose gel electrophoresis for positive-strand MHV-specific RNA. The remaining two-thirds of the sample was reserved for negative-strand RNA analysis. For detection of positive-strand DI RNA, the precipitated RNAs were dissolved in 1× TE containing 0.5% SDS and 50 μg/ml proteinase K (Sigma) and digested at 37° for 30 min. After two phenol/chloroform extractions, the RNA was ethanol precipitated, collected by centrifugation, and resuspended in water. Identical amounts of total RNA from each sample were dissolved in a buffer containing 50% formamide, 4% formaldehyde, 20 m*M* MOPS, heat-denatured at 65° for 15 min, and electrophoresed in 1% agarose gels containing 2.2 *M* formaldehyde. The gels were dried and autoradiographed with X-ray film (Fuji). Quantitative analysis of the replication of positive-strand DI RNA was carried out by scanning autoradiographic images with a ImageMaster DTS laser densitometer (Pharmacia LKB).

Detection of negative-strand DI RNA transcription by competitive RT-PCR

For analysis of negative-strand DI RNA, precipitated RNA representing two-thirds of each culture were dissolved in DNase digestion buffer (40 m*M* Tris–HCl, pH 7.5, 6 m*M* $MgCl_2$, 2 m*M* spermidine, and 10 m*M* NaCl) and digested with 3 U RNase-free DNase (Promega) at 37° for 15 min followed by digestion with 50 μg/ml proteinase K in 0.5% SDS at 37° for 30 min. After two phenol/chloroform extractions, the RNA was ethanol precipitated, collected by centrifugation, and resuspended in water. A reverse-transcription primer, 5′-GGC GTT GTC TAA AGA GAT TTG-3′, which encompasses the junction region between domain II and domain III of DE25 and specifically hybridizes to negative-strand DI RNA at nt 615 to 594 from the 3′ end of the DI RNA (Makino *et al.,* 1988), was used to prime DI RNA cDNA synthesis from intracellular RNA templates. Total RNAs (2.5 μg) from each sample and 180 ng of RT primer were mixed in 15 μl H_2O, heat-denatured at 75° for 10 min and incubated at 42° for 30 min in a final volume of 50 μl of 1× PCR buffer II (Perkin–Elmer Cetus) containing 5 m*M* $MgCl_2$, 1 m*M* of dNTPs, 5 U Moloney murine leukemia reverse transcriptase (MuLV RT, Perkin–Elmer), and 15 U RNasin (Promega). After the RT reaction, 6 μg of RNase A (Sigma) and 2 U RNase T_1 (Calbiochem) were added to each tube

and incubated at 37° for 15 min to completely digest RNA. MuLV RT was inactivated by heating the tubes at 100° for 10 min.

The protocol developed for the quantitative analysis of negative-strand DI RNA by competitive RT-PCR is based on a previously reported method with some minor modifications (Dukas *et al.,* 1993). The 5′ positive-sense primer was identical to the primer used for cDNA synthesis; the sequence of the 3′ negative-sense primer was 5′-GTG ATT CTT CCA ATT GGC-3′, which binds to nt 18 to 1 from the 3′ end of viral genome, yielding a 615-bp PCR fragment of DI RNA. Competitive RT-PCR was carried out in a final volume of 50 μl of 1× PCR buffer II (Perkin–Elmer Cetus) containing 5 m*M* $MgCl_2$, 0.4 m*M* dNTPs, 100 ng of each primer, and 0.5 U *Taq* polymerase in the presence of a 3-μl aliquot of cDNA from the RT reaction and different concentrations of a 510-base internal standard cDNA (competitor cDNA). This competitor cDNA contains the same primer binding sites as cDNA derived from DIssE RNA and a 105-base internal deletion corresponding to nt 593 to 489 from the 3′ end of the viral genome. Thirty cycles of PCR were performed with a denaturation step at 95° for 60 sec, annealing step at 51° for 30 sec, and an elongation step at 72° for 90 sec. The last cycle had an elongation step of 5 min. All reactions were performed in a DNA Thermal Cycler (Perkin–Elmer Cetus). Twenty microliters of PCR products was electrophoresed on a 6% nondenaturing polyacrylamide gel. The gel was stained with ethidium bromide (0.5 μg/ml) for 30 min and photographed with Type 55 positive/negative film (Polaroid). The amplified DNA bands were quantitated by scanning the negative film with a laser densitometer.

Direct sequencing of RT-PCR products

PCR products corresponding to DI RNA (615 bp) were purified by electrophoresis on a 0.8% agarose gel. The DNA bands were excised from the gel and purified with the Geneclean II kit (Bio 101). A sequencing oligonucleotide (5′-TAA GTT GAA AGA GAT TGC-3′) corresponding to positive-strand genomic RNA of JHM at nt 171 to 154 or oligonucleotide (5′-GTG ATT CTT CCA ATT GGC-3′) corresponding to negative-strand RNA at position of nt 18 to 1 from the 3′ end of genome was synthesized and direct sequencing of PCR fragments was performed with the dsDNA cycle sequencing system kit (Life Technologies) following the procedure described by the manufacturer.

RESULTS

Precise localization of host protein binding motif at the 3′ end of JHM genomic RNA

To more precisely localize the protein-binding element we had previously identified within the last 42 nt of the

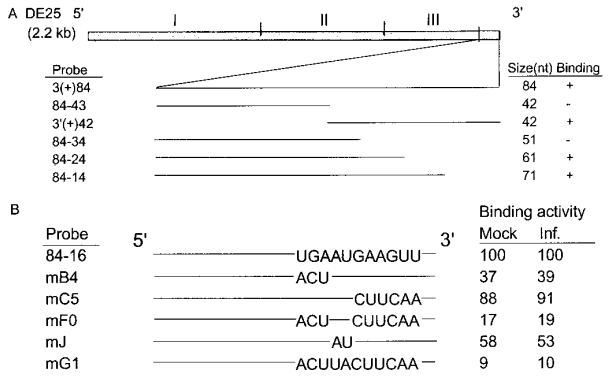

FIG. 1. (A) Schematic diagram of DE25 cDNA, the locations of RNA probes, and summary of RNase T_1 protection/gel mobility shift assays. cDNAs representing various segments of the 3′ end of the genome fused to the T7 promoter were synthesized as described under Materials and Methods. ^{32}P-labeled RNA probes were synthesized by *in vitro* transcription with T7 RNA polymerase. Each probe was named by nucleotide numbers or location within the genomic RNA sequence upstream from the 5′-most A in the poly(A) tail (position 0). For example, 3′(+)42 represents the 42 nt upstream from 0, and probe 84-34 represents a 51-nt sequence from nt 84 to 34 upstream from position 0. The size of each probe is indicated, as the relative position and length. +, formation of an RNase T_1-resistant complex; −, no complex was detected in RNase protection/mobility shift assays. (B) Summary of mutational analysis of 11-nt sequence essential for RNA–protein interaction. Two nanograms of the wild-type 84-16 RNA, corresponding to the 69-nt sequence from nt 84 to 16 from the 3′ end of the genome and encompassing the 11-nt UGAAUGAAGUU, as well as mutant RNA probes with transversion substitutions within this 11-nt region, were tested for the protein-binding ability in RNase protection/gel retardation assay using 7 μg of mock- and JHM-infected cell lysates. The RNA–protein binding activity was quantitated by scanning the ^{32}P-labeled gels with a Betascope blot analyzer. Each number represents the mean of three individual experiments.

MHV genome four ^{32}P-labeled RNA probes (the 84-34, 84-24, 84-16, and 84-14 RNAs), which span nt 84 to 34, 84 to 24, 84 to 16, and 84 to 14, respectively, from the 3′ end of viral genome, were synthesized *in vitro* and tested for the ability to form RNA–protein complexes, using RNase T_1 protection/gel mobility shift electrophoresis. These results are summarized in Fig. 1. Two poorly resolved complexes were observed with the 84-24, 84-16, or 84-14 probes, but no complexes could be detected with the 84-34 RNA (data not shown). To verify the specificity of RNA–protein binding, competition experiments with 75-fold molar excesses of unlabeled specific and nonspecific competitor RNA were performed. One such experiment with the 84-16 probe is shown in Fig. 2. The formation of the complex by the 84-16 RNA was almost completely blocked by a 75-fold molar excess of the unlabeled 84-16 RNA (Fig. 2, lanes 3 and 6), but barely affected by a 75-fold nonspecific competitor tRNA (Fig. 2, lanes 4 and 7). Furthermore, no bands corresponding to the complexes were observed when the 84-16 probe alone was digested with RNase T_1 in the absence of cytoplasmic extract (Fig. 2, lane 1).

These results, coupled with our previous report that

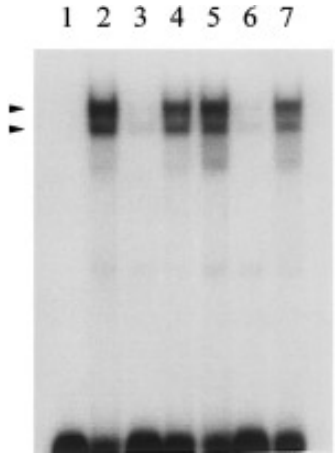

FIG. 2. Specific binding of host cellular proteins to the wild-type 84-16 RNA. Two nanograms of ^{32}P-labeled 84-16 RNA was incubated with 7 μg cytoplasmic extracts from either mock-infected (lanes 2 to 4) or MHV-JHM-infected (lanes 5 to 7) 17Cl-1 cells. The binding mixtures were digested with RNase T_1 (0.00625 U/10 μl) and analyzed by electrophoresis on a 6% nondenaturing polyacrylamide gel. Lane 1, free 84-16 RNA probe; lanes 2 and 5, 84-16 probes incubated with mock- and MHV-infected lysates in the absence of competitor RNA; lanes 3 and 6, 84-16 probes incubated with mock- and MHV-infected lysates in the presence of a 75-fold molar excess of unlabeled specific 84-16 RNA; lanes 4 and 7, 84-16 probes incubated with mock- and MHV-infected lysates in the presence of a 75-fold molar excess of 70 to 90-nt nonspecific tRNA. Arrowheads denote the positions of RNA–protein complexes.

the 84-43 RNA did not have any protein-binding activity (Yu and Leibowitz, 1995), mapped a protein-binding element to a 19-nt sequence from nt 42 to 24 at the 3′ end of JHM genomic RNA. These 19 nt include an 11-nt sequence motif, UGARNGAAGUU (Fig. 1), which is conserved in both the MHV upstream (171-85) and the downstream (42-1) protein-binding regions (Yu and Leibowitz, 1995). To investigate whether this 11-nt sequence is responsible for host protein binding, we compared the ability of wild-type (the 84-16 RNA) and a set of mutant RNA probes to form RNA–protein complexes in the presence of cytoplasmic extracts from mock- and MHV-infected 17Cl-1 cells. A series of cDNAs corresponding to nt 84 to 16 of the wild-type sequence or the mutations shown in Fig. 1 was put under the control of the T7 promoter by PCR. ^{32}P-labeled RNA probes were transcribed from these templates with T7 RNA polymerase; 2 ng of each labeled probe was incubated with cytoplasmic extracts, digested with RNase T_1, and then RNase-resistant RNA–protein complexes were resolved by electrophoresis and visualized by autoradiography. The 84-16 probe formed two poorly resolved complexes in the presence of either mock- or JHM-infected lysate (Fig. 3A, lanes 2 and 3). RNA–protein complexes were barely detectable in reactions containing either mock- or JHM-infected lysates incubated with the mG1 probe in which the entire 11-nt sequence had been mutated (Fig. 3A, lanes 5 and 6). Quantitative analysis indicated that the protein-binding activity of the mG1 probe was only 9–10% of the wild-type 84-16 probe. Less extensive mutations within this 11-nt sequence, such as those contained in the mB4, mC5, and mF0 RNA probes, resulted in variable decreases in RNA–protein complex formation (Fig. 3B, lanes 4 to 12). The mB4 RNA expressed 39% of the protein-binding activity seen with the wild-type RNA, while the mC5 RNA with a mutation of the last 6-nt GAAGUU sequence maintained 90% of the protein-binding activity (Fig. 1B). However, the contribution of this sequence to protein binding could be observed when this mutation (mC5) was combined with the mutation contained in mB4 (mF0). The mF0 RNA had 17% of the wild-type activity, considerably less than that observed with either of the mutant RNA probes (mB4 and mC5) carrying the mutations separately. The complexes formed by the wild-type and mutant probes with cytoplasmic extracts from mock- and JHM-infected cells had identical electrophoretic mobilities (Figs. 3A and 3B). In addition, for each probe the efficiency of complex formation was similar with mock-infected and MHV-infected lysates. These results confirmed that the sequence UGAAUGAAGUU at the 3′ end of genomic RNA of MHV is an important determinant of specific binding of host cellular proteins.

Characterization of RNA binding proteins by UV-induced cross-linking

To characterize the proteins bound to the wild-type and mutant RNA probes and determine their molecular weights, ^{32}P label was transferred from RNA probes to

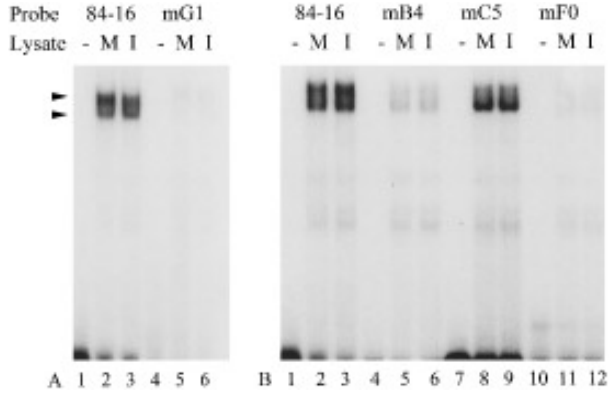

FIG. 3. Mutational analysis of 11-nt sequence required for RNA–protein binding. RNA–protein binding reactions were carried out as described in the legend to Fig. 2. (A) Lanes 1 and 4, free 84-16 RNA and mG1 RNA with a mutation of 11-nt UGAAUGAAGUU in the absence of cell lysates; lanes 2 and 5, 84-16 and mG1 RNAs incubated with mock-infected lysates; lanes 3 and 6, 84-16 and mG1 RNAs incubated with JHM-infected lysates. (B) Lanes 1, 4, 7, and 10, free 84-16 probe, mB4 probe with a mutation of 3-nt UGA, mC5 probe with a mutation of 6-nt GAAGUU, mF0 probe with a mutation of both UGA and GAAGUU in the absence of cell lysates, respectively; lanes 2, 5, 8, and 11, 84-16, mB4, mC5, and mF0 probes incubated with mock-infected lysates, respectively; lanes 3, 6, 9, and 12, 84-16, mB4, mC5, and mF0 probes incubated with JHM-infected lysates, respectively.

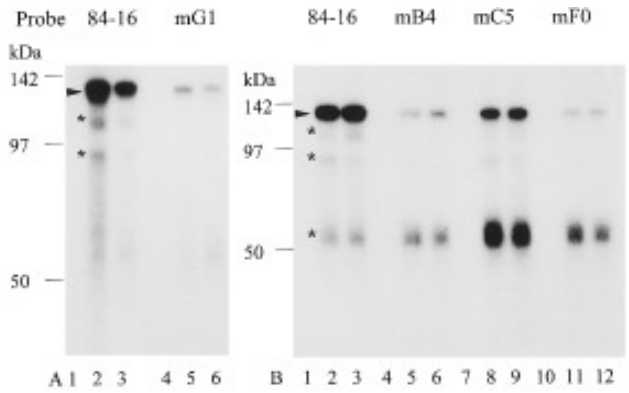

FIG. 4. Identification of host cellular proteins binding to the 11-nt motif by UV cross-linking. RNA–protein binding reactions using labeled RNA were carried out as described in the legend to Fig. 2. Following incubation with RNase T_1 (0.00625 U/10 μl), ^{32}P-labeled RNA–protein complexes were UV cross-linked and digested with RNase A prior to 10% SDS–PAGE. The experiments shown in A and B were performed with two different preparations of cytoplasmic lysates. A highly labeled protein of 120 kDa is indicated by arrowheads; minor proteins are indicated by asterisks. Prestained molecular weight standards (Bio-Rad) were used as markers. (A) Lanes 1 and 4, free 84-16 and mG1 RNA probes in the absence of cell lysates; lanes 2 and 5, 84-16 and mG1 RNAs incubated with mock-infected lysates; lanes 3 and 6, 84-16 and mG1 RNAs incubated with JHM-infected lysates. (B) Lanes 1, 4, 7, and 10, free 84-16, mB4, mC5, and mF0 probes in the absence of cell lysates; lanes 2, 5, 8, and 11, 84-16, mB4, mC5, and mF0 probes incubated with mock-infected lysates, respectively; lanes 3, 6, 9, and 12, 84-16, mB4, mC5, and mF0 probes incubated with JHM-infected lysates, respectively.

proteins bound directly to these RNAs by UV irradiation. After limited RNase T_1 digestion, RNA binding reaction mixtures were irradiated with UV for 30 min and then completely digested with RNase A. Proteins to which ^{32}P label was transferred by UV cross-linking were analyzed by SDS-polyacrylamide gel electrophoresis (PAGE). In the absence of cytoplasmic extracts, no bands were observed after UV irradiation of any RNA probe (Fig. 4A, lanes 1 and 4, and Fig. 4B, lanes 1, 4, 7, and 10). The RNA–protein complex formed with the 84-16 RNA contains approximately four host polypeptides, a highly labeled protein of 120 kDa, and three minor species with sizes of 103, 81, and 55 kDa (Figs. 4A, and Fig. 4B, lanes 2 and 3). Incubation of mG1 RNA probe, which contained an 11-nt mutation, with cell lysates, decreased the amount of the 103- and 80-kDa proteins in the complex to undetectable levels, and strongly reduced the binding of the 120-kDa protein (Fig. 4A, lanes 4 and 5). The protein profiles of RNA–protein complexes formed with mB4 and mF0 RNA probes were similar to that of mG1 probe (Fig. 4B, lanes 5, 6, 11, and 12), while the protein profile of the complex formed with mC5 probe was similar to that of wild-type 84-16 probe (Fig. 4B, lanes 8 and 9). The 55-kDa protein seems to be a relatively nonspecific binding protein; its presence in the complex seems not affected by mutations which decrease the binding of the other proteins in the complex. In addition, with some preparations of cytoplasmic extract the 55-kDa protein is barely observed in the complex (compare lanes 2 in Figs. 4A and 4B).

Effects of mutation at the protein-binding motif on replication of positive-strand DI RNA

Having identified the 11-nt sequence at position 36-26 nt as a required motif in the 3′ protein-binding element, we investigated the role this protein-binding motif might play in the viral life cycle, particularly in RNA replication. The plasmid DE25, which carries a 2.2-kb cDNA insert of the MHV-JHM DI RNA DIssE (Makino and Lai, 1989), was used as the wild-type template for the introduction of mutations into the protein-binding element by site-directed mutagenesis. DE25-derived mutants containing the same mutations utilized in our protein-binding experiments were constructed, and DI RNAs were transcribed *in vitro* and transfected into host 17Cl-1 cells infected with MHV-JHM as helper virus 1 hr prior to transfection. Viral replication was assayed by labeling replicating DI RNA with ^{32}Pi in the presence of actinomycin D and directly analyzing the RNA by gel electrophoresis. We have elected to use this assay rather than an assay based on hybridization to avoid potential confusion from input-transfected RNA. No DI RNA was observed when host cells were only infected with helper virus in the absence of transfected DE25 derived RNA (Fig. 5A, lane 1). Replication of wild-type DE25 and mG1 DI RNA was easily detected (Fig. 5A, lanes 2 and 3), while replication of mB4 and mC5 DI RNA was at barely observable levels (Fig. 5A, lanes 4 and 5).

The levels of positive-strand DI RNAs replication for the experiment shown in Fig. 5A were measured as described under Materials and Methods. Replication of mG1 DI RNA (which contains a completely mutagenized 11-nt motif), mB4 DI RNA (which contains a UGA mutation in positions 36-34 nt), and mC5 DI RNA (which contains a GAAGUU mutation in positions 31-26 nt) were 63, 28, and 21% of wild-type DE25 RNA (Fig. 5C). The replication level of mG1 RNA which carried a completely mutagenized 11-nt motif was higher than that of either mB4 or mC5 RNAs containing partial mutations of this motif, a result which surprised us. As coronaviruses undergo recombination at high frequency (Liao and Lai, 1992), we determined if the mG1 RNA sequence was maintained or if the replicated mutant DI RNA had been converted to the wild-type RNA sequence. cDNAs were synthesized using a reverse-transcription primer complementary to negative-strand DI RNA and RNA templates prepared from each of the transfections described above; these cDNAs were amplified by PCR and directly sequenced. As indicated in Fig. 5B, transcription of negative-strand RNA from each transfected DI RNA, DE25, mG1, mB4, and mC5 (lanes 2 to 5), was observed, but not from RNA isolated from nontransfected JHM-infected cells (lane 1).

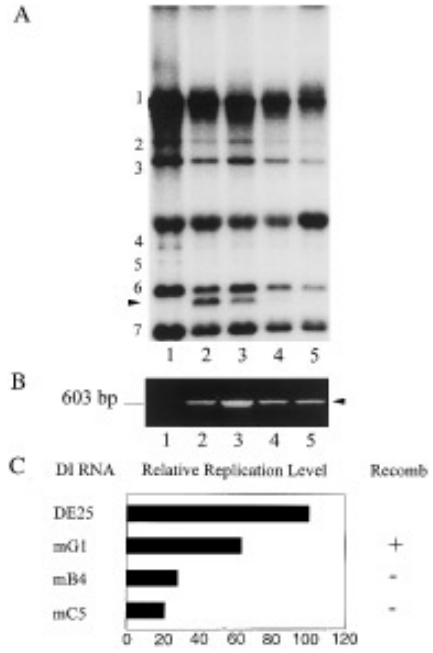

FIG. 5. (A) Replication of wild-type DE25 and DE25-derived mutants in DI RNA-transfected and JHM-infected cells. Each 1.5-μg *in vitro* synthesized DI RNA was mixed with 15 μg cellFECTIN and transfected into JHM-infected cells. Virus-specific and replicated DI RNAs were labeled with ^{32}Pi for 2 hr from 7.5 to 9.5 hr postinfection in the presence of actinomycin D. Total RNA (2.5 μg) from each sample was electrophoresed on a 1% denaturing agarose gel containing formaldehyde. Lane 1, no DI RNA; lane 2, DE25; lane 3, mG1; lane 4, mB4; lane 5, mC5 DI RNA. The replicated DI RNA is indicated by an arrowhead and the MHV-JHM-specific mRNAs were numbered from 1 to 7. (B) Transcription of negative-strand wild-type DE25 and DE25-derived mutants in DI RNA-transfected and JHM-infected cells. DI RNA cDNAs were synthesized from intracellular RNAs by MuLV reverse transcriptase using a primer which binds only negative-strand DI RNA. A 615-bp DNA fragment was amplified by subsequent PCR, resolved on 0.8% agarose gel, and stained with ethidium bromide. Lane 1, no DI RNA transfection; lane 2, DE25; lane 3, mG1; lane 4, mB4; lane 5, mC5 DI RNA. The arrowhead denotes amplified 615-bp DNA fragment derived from negative-strand DI RNA. PhiX 174 DNAs digested with *Hae*III (Promega) were used as markers. (C) Quantitative analysis of DI RNA replication and summary of recombination of mutant DI RNAs during replication. Replication of DI RNAs was quantitated by scanning the autoradiographic film from (A) with a laser densitometer and expressed relative to the percentage of DE25 replication. Detection of recombination was performed by direct sequencing of RT-PCR fragments derived from negative strand DI RNA. +, mutated sequence was converted to wild-type sequence; −, mutated sequence was not converted to wild-type sequence.

The sequencing data demonstrated that the mG1 RNA mutated sequence, ACUUACUUCAA, had been converted to the wild-type sequence, UGAAUGAAGUU, presumably via recombination with helper virus. However, both the mB4 and the mC5 DI RNAs maintained their mutated sequence in this experiment (Fig. 5C).

We repeated this experiment but also included a DI RNA containing a mutation outside the 11-nt protein-binding motif. Different results were obtained, as shown in Fig. 6A. The replication of mG1 RNA was barely detectable (lane 3), while replication of mB4 and mC5 RNA almost reached the level of wild-type DE25 RNA (lanes 4 to 5). Quantitative analysis indicated that replication of positive-strand mG1 RNA was reduced to 27% of that observed for DE25 RNA, while mB4 and mC5 RNA replication was 96 and 89% of DE25, respectively (Fig. 6C). These results differed from those shown in Fig. 5, where the replication of mB4 and mC5 RNA were strongly reduced relative to wild type, while mG1 RNA replication was only moderately decreased compared to DE25 RNA. Again, RT-PCR demonstrated the synthesis of negative-strand DI RNA from each transfected DI RNA (Fig. 6B). Sequencing data revealed that all three DI RNAs, mG1, mB4 and mC5, had been converted to the wild-type sequence, presumably by recombination (Fig. 6C). Despite recombination of mG1 DI RNA with helper virus, a significant decrease of mG1 RNA synthesis was observed in this experiment (Fig. 6A, lane 3). A DI RNA (mD6) containing a 3-nt mutation from nt 177 to 175 at the 3′ end of genome and located upstream of both known 3′ protein-binding elements was also included in this experiment to see if a DI RNA carrying a mutation which is predicted to have little or no effect on protein-binding or replication would achieve similar replication levels as DE25 without undergoing recombination. As shown in Fig. 6A, lane 6, mD6 RNA replicated at the same level of wild-type DE25

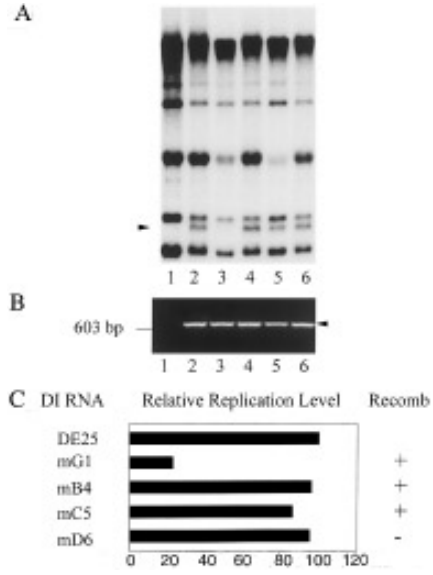

FIG. 6. (A) Replication of wild-type DE25 and DE25-derived mutants in DI RNA-transfected and JHM-infected cells. The assay was carried out as described in the legend to Fig. 5 (A). Total RNA (1.5 μg) from each sample were electrophoresed on 1% formaldehyde–agarose gel. Lane 1, no DI RNA; lane 2, DE25; lane 3, mG1; lane 4, mB4; lane 5, mC5; lane 6, mD6 DI RNA. The replicated DI RNA is indicated by an arrowhead. (B) Transcription of negative-strand wild-type DE25 and DE25-derived mutants in DI RNA-transfected and JHM-infected cells. The assay was performed as described in the legend to Fig. 5 (B). Lane 1, no DI RNA; lane 2, DE25; lane 3, mG1; lane 4, mB4; lane 5, mC5; lane 6, mD6 DI RNA. (C) Quantitative analysis of DI RNA replication and summary of recombination of mutant DI RNAs during replication. The data were expressed as described in the legend to Fig. 5 (C).

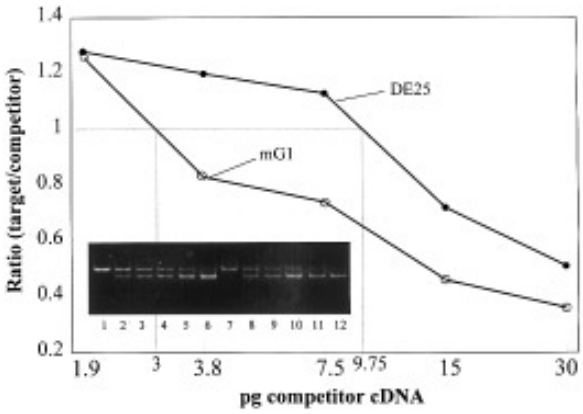

FIG. 7. Quantitative analysis of transcription of negative-strand DE25 and mG1 DI RNA by competitive RT-PCR. Total RNA (2.5 μg) from DE25 (lanes 1 to 6) and mG1 (lanes 7 to 12) transfected cells were reverse transcribed and subjected to 30 cycles of PCR amplification in the presence of increasing amounts of competitor cDNA (lanes 1 and 7, 0; lanes 2 and 8, 1.875 pg; lanes 3 and 9, 3.75 pg; lanes 4 and 10, 7.5 pg; lanes 5 and 11, 15 pg; lanes 6 and 12, 30 pg). Target PCR fragment with size of 615 bp (top bands) and competitor PCR fragment with size of 510 bp (bottom bands) were resolved on a 6% native polyacrylamide gel. The ratios of target PCR products formed in each mixture to competitor PCR products are calculated and plotted versus the relative abundance of the competitor cDNA in each mixture.

RNA while still maintaining the mutant sequence (Fig. 6C). We interpret these results as providing an indication that the 11-nt sequence UGAAUGAAGUU at the 3′ end of genomic RNA of MHV is required for the efficient replication of DI RNA, although high rates of recombination with helper virus appear to preclude unequivocally, demonstrating this point.

Effects of mutation at the protein-binding motif on transcription of negative-strand DI RNA

To determine if the mutation in the mG1 DI RNA differentially affects negative-strand or positive-strand RNA synthesis, competitive RT-PCR was performed to quantitate negative-strand synthesis of DE25 and mG1 DI RNA. To allow a comparison of the synthesis of positive- and negative-strand DI RNAs from the same samples, aliquots of the ^{32}P-labeled viral RNAs shown in Fig. 6 were also used for detection of negative-strand DI RNA, except an additional step of DNase digestion was included. cDNA was synthesized by reverse transcriptase using the positive-sense RT primer spanning the junction of DI RNA regions II and III. After the RT reaction, increasing amounts of competitor cDNA were added to each aliquot of samples and cDNAs were coamplified by PCR. Size-separated PCR fragments (615 bp for DI RNA cDNA and 510 bp for competitor cDNA) were resolved by gel electrophoresis. As shown in Fig. 7, there is a linear decrease in the coamplification of negative strand DI RNA with increasing concentrations of standard cDNA and a linear response between the amount of input competitor cDNA and PCR product. The ratio of DI RNA PCR (target PCR) to competitor PCR product was calculated and plotted. Results indicated that a ratio of one is obtained at a value of 9.75 for DE25 cDNA, whereas the same ratio is obtained at a value of 3 for mG1 cDNA. Thus a 3.25-fold difference between the two samples was demonstrated. These results indicated that synthesis of negative-strand mG1 RNA is approximately 31% of wild-type DE25 RNA, which is similar to the effect on positive-strand replication of mG1 RNA relative to the wild-type DE25 (27%, Fig. 6C).

Kinetic analysis of DI RNA replication and recombination

In an attempt to detect when recombination might occur, DE25 RNA and mG1 RNA were transfected into cells and viral RNA were labeled with ^{32}Pi at different times, from 5.5 to 7.5 hr and from 7.5 to 9.5 hr postinfection (p.i). When cells were labeled with ^{32}Pi from 5.5 to 7.5 hr p.i., no replication of either DI RNA was observed and replication of helper virus mRNAs was just beginning (Fig. 8A, lanes 2 and 3). When ^{32}Pi labeling was conducted from 7.5 to 9.5 hr, both DE25 and mG1 RNA were replicating, with the latter reduced by 38% compared to the former (Fig. 8A, lanes 5 and 6). Again sequencing data from RT-PCR demonstrated that at relatively early times of infection (5.5 to 7.5 hr p.i.), when replication of

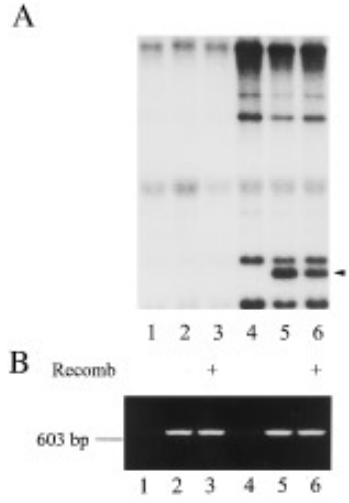

FIG. 8. (A) Replication of DE25 and mG1 DI RNA at different time postinfection. Virus-specific and replicated DI RNAs were labeled with ^{32}Pi for 2 hr from 5.5 to 7.5 hr (lanes 1 to 3) and from 7.5 to 9.5 hr postinfection (lanes 4 to 6) in the presence of actinomycin D. Total RNA (2.5 μg) from each sample was electrophoresed on a 1% denaturing agarose gel containing formaldehyde. Lanes 1 and 4, no DI RNA; lanes 2 and 5, DE25 DI RNA; lanes 3 and 6, mG1 DI RNA. The replicated DI RNA is indicated by an arrowhead. (B) Synthesis of negative-strand DI RNA and recombination of mG1 mutant at different time postinfection. Detection of negative-strand DI RNA was conducted as described in the legend to Fig. 5 (B). Lanes 1 and 4, no DI RNA; lanes 2 and 5, DE25; lanes 3 and 6, mG1 DI RNA. Recombination was assayed as described in the legend to Fig. 5 (C).

positive-strand DI RNA was barely observed, synthesis of negative-strand mG1 RNA could be detected and the recombination between transfected mG1 RNA and helper virus had already taken place (Fig. 8B).

DISCUSSION

Our approach to studying the mechanism of MHV RNA replication is to precisely identify the host and/or viral protein-binding element at the 3′ end of genomic RNA, to examine the requirement for protein binding to this site for viral replication, and to determine the identity and function of the protein(s) which bind to this element. We have presented evidence here that a host protein-binding site maps to a 19-nt sequence from nt 42 to nt 24 at the 3′ end of genomic RNA of MHV, and that mutation of the 11-nt sequence UGAAUGAAGUU within this region, prevented binding of cellular proteins *in vitro,* confirming that this 11-nt sequence is an important determinant for RNA–protein complex formation. This sequence is fully conserved among MHV strains (Parker and Masters, 1990).

The large size of MHV genome RNA (31 kb) has to date prevented the construction of its full-length, infectious cDNA clone. Thus, cDNA clones corresponding to replication competent MHV DI RNAs have been created and extensively utilized to study MHV replication in the presence of helper virus (Brian *et al.,* 1994; Kim *et al.,* 1993; Lin and Lai, 1993; Lin *et al.,* 1994; van der Most *et al.,* 1994). Such a strategy has also been applied to identify *cis*-acting replication signals in other positive-strand virus such as Sindbis virus (Levis *et al.,* 1986) and brome mosaic virus (French and Ahlquist, 1987). Although the availability of a MHV DI RNA cDNA (DE25) allowed us to assess the effect of the protein-binding motif on DI RNA replication, detection of DI RNA replication *in vivo* in the presence of helper virus was complicated by recombination between transfected DI RNA and helper virus, resulting in considerable variability from experiment to experiment. Mutations within the 11-nt motif which disrupt RNA–protein interactions were introduced into DI RNA. The synthesis of positive-strand mG1 DI RNA carrying a completely mutagenized motif was only 27 to 63% of wild-type DE25 RNA, even though the mutation sequence was repaired by recombination with helper virus during the course of the experiment. Replication of positive-strand DI RNA carrying less extensive mutations within the protein-binding motif, i.e., mB4 (UGA) and mC5 (GAAGUU), was dependent on recombination events during infection. In the experiment where reversion to the wild-type sequence did not take place (Fig. 5), the replication level of either DI RNA was greatly decreased compared to that of wild type. However, there was not an absolute correlation between the effect of a given mutation on protein-binding activity and RNA replication. Among several mutant RNA probes, the mC5 mutation had a minimal effect on protein-binding activity (Fig. 1). However, in the experiment shown in Fig. 5, where recombination did not rescue the mutation, it nevertheless substantially decreased DI replication. Thus, the 11-nt sequence may contain two partially overlapping functional elements, one of which is necessary for replication independent of its effect on protein binding. In experiments where recombination events had restored the wild-type sequence, mB4 and mC5 replicated to levels similar to wild-type DE25 RNA. mD6 RNA, containing a 3-nt mutation located upstream of both known 3′ protein-binding elements and predicted to have little or no effect on protein-binding or replication, replicated as efficiently as DE25 RNA without undergoing recombination. This indicated that recombination is not an indispensable event for every transfected mutant RNA which replicates as well as wild type, but depends on the site of the introduced mutation. Although replication of mG1 RNA varied greatly from one experiment to another, RT-PCR sequencing data from three separate experiments all demonstrated the conversion of transfected DI RNA to the wild-type sequence, providing an indication that the conserved 11-nt sequence located from nt 36 to 26 at the 3′ end of genomic RNA of MHV is strongly selected during replication. These results also raise special cautions in the interpretation of data from studies of coronavirus DI RNA replication when RT-PCR sequencing of DI RNA is not performed in parallel to verify the maintenance of the introduced mutation.

Recently published work demonstrated that only 55 nt from the 3′ end of genome is required for negative-strand DI RNA synthesis (Lin *et al.,* 1994). These 55 nt encompass the 11-nt protein-binding motif we identified. Our results are consistent with this observation, in that the mG1 mutation resulted in a parallel decrease in both positive- and negative-strand RNA synthesis. The complicating effects of recombination combined with the temporal linkage of positive- and negative-strand synthesis (Sawicki and Sawicki, 1990) preclude definitively determining if the primary requirement for this motif is for negative-strand synthesis and its effect on positive-strand replication is indirect or if it directly effects positive-strand synthesis as well.

At present we are unsure whether the related sequence UGAGAGAAGUU, located 129-nt from the 3′ termini of viral genome within the upstream (171-85) 3′ protein-binding element, plays any role in viral replication. The data we have presented here, indicating that the mutagenized 11-nt motif in the mG1 RNA probe has a small amount of residual activity of protein-binding, does not let us distinguish between two alternative hypotheses. In the first hypothesis, the upstream protein-binding motif does not function in RNA replication; the residual low-level protein-binding activity of the 3′ most motif allows for a low level of replication sufficient for rescue of the mutated DI by recombination with helper virus.

The second hypothesis invokes a role for the upstream protein-binding motif in replication. The upstream element would provide a degree of redundancy for the MHV replicon and allows replication to proceed, albeit less efficiently, if the downstream nt 36-26 protein-binding element is inactivated. The sequencing data demonstrating that all transfected mG1 DI RNA was converted to the wild-type sequence by recombination suggest that this upstream protein-binding element, if it does have a role in MHV RNA synthesis, could not completely compensate for the mutation in the mG1 RNA. Further studies of the effect of mutations in upstream (175-85) protein-binding element or in both protein-binding elements will help answer this question.

Sequences at the 3′ end of genomic RNA are strongly conserved amongst MHV strains (Parker and Masters, 1990); therefore, it seems likely that sequences flanking the 11-nt protein-binding motif might also play a role in viral replication. The particular role of these sequences in replication is unknown but could include stabilizing secondary structures at the 3′ end of genome as well as directly interacting with host or viral proteins.

Host cell proteins binding to either the 3′ or the 5′ end of genome RNA have been reported in positive-strand coronavirus (Furuya and Lai, 1993; Yu and Leibowitz, 1995), hepatitis A virus (Nuesch *et al.,* 1993), hepatitis C virus (Yen *et al.,* 1995), poliovirus (Andino *et al.,* 1990, 1993; Del Angel *et al.,* 1989), rhinovirus (Todd *et al.,* 1995), and rubella virus (Nakhasi *et al.,* 1991) as well as in negative-strand measles virus (Leopardi *et al.,* 1993). Host proteins were also found to bind to the 3′ end of the full-length negative-sense Sindbis virus-specific RNA (Pardigon and Strauss, 1992), suggesting the involvement of host proteins in the life cycle of a number of diverse viruses. A 55-kDa host cell protein has been shown to bind to positive-sense RNA corresponding to nt 56 to 112 from the 5′ end of genomic RNA of MHV (Furuya and Lai, 1993). The association of host proteins with viral RNA replication has been reported for some positive-strand RNA viruses, such as brome mosaic virus (Quadt *et al.,* 1993) and poliovirus (Andino *et al.,* 1990, 1993). In brome mosaic virus, a host protein of 45 kDa bound to the RNA-dependent RNA polymerase (RDRP) was determined to be the barley analog of eIF-3 subunit p41, but the interaction of this protein with genomic RNA was not detected (Quadt *et al.,* 1993). In poliovirus, the binding of a 36-kDa host protein associated with RDRP to 5′-most 90 nt of genomic RNA was observed, but the identity of this host protein was not established (Andino *et al.,* 1990, 1993). At present little is known regarding host and virus-specific proteins in the RDRP complex necessary for initiation of negative-strand RNA synthesis during MHV RNA replication, due in part to a lack of characterization of MHV RDRP and the unavailability of a reproducible and efficient system to study viral RNA replication *in vitro.* The results of our UV cross-linking experiment showed that RNA probe containing the 11-nt sequence binds four host proteins with sizes of 120, 103, 81, and 55 kDa. Mutations which disrupt RNA–protein complex formation appeared to result in the disappearance of two proteins of 103 and 80 kDa from the complex and dramatically decreased the binding of a highly labeled 120-kDa protein, suggesting a correlation between the presence of these protein components in the RNA–protein complex and DI RNA replication. The identity and biological functions of these proteins in viral replication remains to be established.

All of our RNase protection/gel mobility shift and UV cross-linking experiments to date have failed to demonstrate binding of any virus-specific protein to this 11-nt sequence, a result which puzzles us. Yet the MHV RDRP must recognize the 3′ region of the genome to initiate negative-strand RNA transcription. This may be an indication that viral proteins do not bind directly to the genomic RNA, but associate with protein-binding elements within genomic RNA via protein–protein interactions and thus could not be detected by the UV cross-linking assay. Alternatively, the binding affinity of viral protein to RNA could be sufficiently low that the RNA–protein complex formed with MHV polymerase proteins is not resistant to RNase T_1 digestion under any of the conditions we used.

An intriguing question raised by the above results is how the binding of host proteins to the conserved 11-nt sequence at the 3′ end of genome affects viral replication and what the identities of these host proteins are. Future studies will be directed to determine the identity of the host cellular proteins associated to the 11-nt motif in viral replication.

ACKNOWLEDGMENTS

We thank Dr. Shinji Makino of University of Texas at Austin for kindly providing the DE25 plasmid and Dr. Madeleine Duvic of Department of Dermatology for valuable advice on competitive RT-PCR. We thank all members of the Leibowitz laboratory for helpful discussions. This work was supported in part by National Multiple Sclerosis Society Research Grant RG 2203-A-5.

REFERENCES

Andino, R., Rieckhof, G. E., and Baltimore, D. (1990). A functional ribonucleoprotein complex forms around the 5′ end of poliovirus RNA. *Cell* 63, 369–380.

Andino, R., Rieckhof, G. E., Achacoso, P. L., and Baltimore, D. (1993). Poliovirus RNA synthesis utilizes an RNP complex formed around the 5′ end of viral RNA. *EMBO J.* 12, 3587–3598.

Baric, R. S., Stohlman, S. A., and Lai, M. M. C. (1983). Characterization of replicative intermediate RNA of mouse hepatitis virus: Presence of leader RNA sequences on nascent chains. *J. Virol.* 48, 633–640.

Brian, D. A., Chang, R. Y., Hofmann, M. A., and Sethna, P. B. (1994). Role of subgenomic minus-strand RNA in coronavirus replication. *Arch. Virol.* 9(Suppl.), 173–180.

Del Angel, R. M., Papavassiliou, A. G., Fernandez-Tomas, C., Silverstein, S. J., and Racaniello, V. R. (1989). Cell proteins bind to multiple sites within the 5′ untranslated region of poliovirus RNA. *Proc. Natl. Acad. Sci. USA* 86, 8299–8303.

Dukas, K., Sarfati, P., Vaysse, N., and Pradayrol, L. (1993). Quantitation of changes in the expression of multiple genes by simultaneous polymerase chain reaction. *Anal. Biochem.* 215, 66–72.

French, R., and Ahlquist, P. (1987). Intercistronic as well as terminal sequences are required for efficient amplification of brome mosaic virus. *J. Virol.* 61, 1457–1465.

Furuya, T., and Lai, M. M. C. (1993). Three different cellular proteins bind to complementary sites on the 5′-end-positive and 3′-end-negative strands of mouse hepatitis virus RNA. *J. Virol.* 67, 7215–7222.

Kim, Y. N., Jeong, Y. S., and Makino, S. (1993). Analysis of *cis*-acting sequences essential for coronavirus defective interfering RNA replication. *Virology* 197, 53–63.

Lai, M. M. C. (1990). Coronavirus: Organization, replication and expression of genome. *Annu. Rev. Microbiol.* 44, 303–333.

Lai, M. M. C., Brayton, P. R., Armen, R. C., Patton, C. D., Pugh, C., and Stohlman, S. A. (1981). Mouse hepatitis virus A59: mRNA structure and genetic localization of the sequence divergence from hepatotropic strain MHV-3. *J. Virol.* 39, 823–834.

Leibowitz, J. L., and DeVries, J. R. (1988). Synthesis of virus-specific RNA in permeabilized murine coronavirus-infected cells. *Virology* 166, 66–75.

Leibowitz, J. L., Wilhelmsen, K. C., and Bond, C. W. (1981). The virus specific intracellular RNA species of two murine coronaviruses: MHV-A59 and MHV-JHM. *Virology* 114, 39–51.

Leibowitz, J. L., Zoltick, P. W., Holmes, K. V., Oleszak, E. L., and Weiss, S. R. (1990). Murine coronavirus RNA synthesis. *In* "New Aspects of Positive-Strand RNA Virus" (M. A. Brinton and F. X. Heinz, Eds.), pp. 67–74. Am. Soc. Microbiol. Washington, DC.

Leopardi, R., Hukkanen, V., Vainionpaa, R., and Salmi, A. A. (1993). Cell proteins bind to sites within the 3′ noncoding region and the positive-strand leader sequence of measles virus RNA. *J. Virol.* 67, 785–790.

Levis, R., Weiss, B. W., Tsiang, M., Huang, H., and Schlesinger, S. (1986). Deletion mapping of Sindbis virus DI RNAs derived from cDNAs defines the sequences essential for replication and packaging. *Cell* 44, 137–145.

Liao, C. L., and Lai, M. M. C. (1992). RNA recombination in a coronavirus: Recombination between viral genomic RNA and transfected RNA fragments. *J. Virol.* 66, 6117–6124.

Lin, Y. J., and Lai, M. M. C. (1993). Deletion mapping of a mouse hepatitis virus defective interfering RNA reveals the requirement of an internal and discontiguous sequence for replication. *J. Virol.* 67, 6110–6118.

Lin, Y. J., Liao, C. L., and Lai, M. M. C. (1994). Identification of the *cis*-acting signal for minus-strand RNA synthesis of a murine coronavirus: Implications for the role of minus-strand RNA in RNA replication and transcription. *J. Virol.* 68, 8131–8140.

Makino, S., and Lai, M. M. C. (1989). High-frequency leader sequence switching during coronavirus defective interfering RNA replication. *J. Virol.* 63, 5285–5292.

Makino, S., Joo, M. S., and Makino, J. K. (1991). A system for study of coronavirus mRNA synthesis: A regulated, expressed subgenomic defective interfering RNA results from intergenic site insertion. *J. Virol.* 65, 6031–6041.

Makino, S., Shieh, C. K., Soe, L. H., Baker, S. C., and Lai, M. M. C. (1988). Primary structure and translation of a defective interfering RNA of murine coronavirus. *Virology* 166, 550–560.

Nakhasi, H., Cao, X. Q., Rouault, T. A., and Liu, T. Y. (1991). Specific binding of host cell proteins to the 3′-terminal stem-loop structure of rubella virus negative-strand RNA. *J. Virol.* 65, 5961–5967.

Nuesch, J. P. F., Weitz, M., and Siegl, G. (1993). Proteins specifically binding to the 3′ untranslated region of hepatitis A virus RNA in persistently infected cells. *Arch. Virol.* 128, 65–79.

Pardigon, N., and Strauss, J. H. (1992). Cellular proteins bind to the 3′ end of Sindbis virus minus-strand RNA. *J. Virol.* 66, 1007–1015.

Parker, M. M., and Masters, P. S. (1990). Sequence comparison of the N genes of five strains of the coronavirus mouse hepatitis virus suggests a three domain structure for the nucleocapsid protein. *Virology* 179, 463–468.

Quadt, R., Kao, C. C., Browning, K. S., Hershberger, R. P., and Ahlquist, P. (1993). Characterization of a host protein associated with brome mosaic virus RNA-dependent RNA polymerase. *Proc. Natl. Acad. Sci. USA* 90, 1498–1502.

Sawicki, S. G., and Sawicki, D. L. (1990). Coronavirus transcription: Subgenomic mouse hepatitis virus replicative intermediates function in RNA synthesis. *J. Virol.* 64, 1050–1056.

Schaad, M. C., and Baric, R. S. (1994). Genetics of mouse hepatitis virus transcription: Eevidence that subgenomic negative strands are functional templates. *J. Virol.* 68, 8169–8179.

Soe, L. H., Shieh, C. K., Baker, S. C., Chang, M. F., and Lai, M. M. C. (1987). Sequence and translation of the murine coronavirus 5′ end genomic RNA reveals the N-terminal structure of the putative RNA polymerase. *J. Virol.* 61, 3968–3976.

Spaan, W. J., Cavanagh, D., and Horzinek, M. C. (1988). Coronaviruses: Structure and genome expression. *J. Gen. Virol.* 69, 2939–2952.

Spaan, W. J., Rottier, P. J., Horzinek, M. C., and Vander Zeust, B. A. (1982). Sequence relationships between the genome and the intracellular RNA species 1, 3, 6, and 7 of mouse hepatitis virus strain A59. *J. Virol.* 42, 432–439.

Todd, S., Nguyen, J. H. C., and Semler, B. L. (1995). RNA–protein interactions directed by the 3′ end of human Rhinovirus genomic RNA. *J. Virol.* 69, 3605–3614.

van der Most, R. G., de Groot, R. J., and Spaan, W.J.M. (1994). Subgenomic RNA synthesis directed by a synthetic defective interfering RNA of mouse hepatitis virus: A study of coronavirus transcription initiation. *J. Virol.* 68, 3656–3666.

Yen, J. H., Chang, S. C., Hu, C. R., Chu, S. C., Lin, S. S., Hsieh, Y. S., and Chang, M.F. (1995). Cellular proteins specifically bind to the 5′-noncoding region of hepatitis C virus RNA. *Virology* 208, 723–733.

Yu, W., and Leibowitz, J. L. (1995). Specific binding of host cellular proteins to multiple sites within the 3′ end of mouse hepatitis virus genomic RNA. *J. Virol.* 69, 2016–2023.